Supplementary figures for

Biointeractions of ultrasmall glutathione-coated gold nanoparticles: effect of small size variations

Alioscka A. Sousa*[,§], Sergio A. Hassan[#], Luiza L. Knittel[§], Andrea Balbo[†], Maria A. Aronova[†], Patrick H. Brown[†], Peter Schuck[†], Richard D. Leapman*[,†]

§ Department of Biochemistry, Federal University of São Paulo, São Paulo, SP 04044, Brazil.

Center for Molecular Modeling, DCB/CIT, National Institutes of Health, Bethesda, MD, USA.

† National Institute of Biomedical Imaging and Bioengineering, National Institutes of Health, Bethesda, MD 20892, USA.

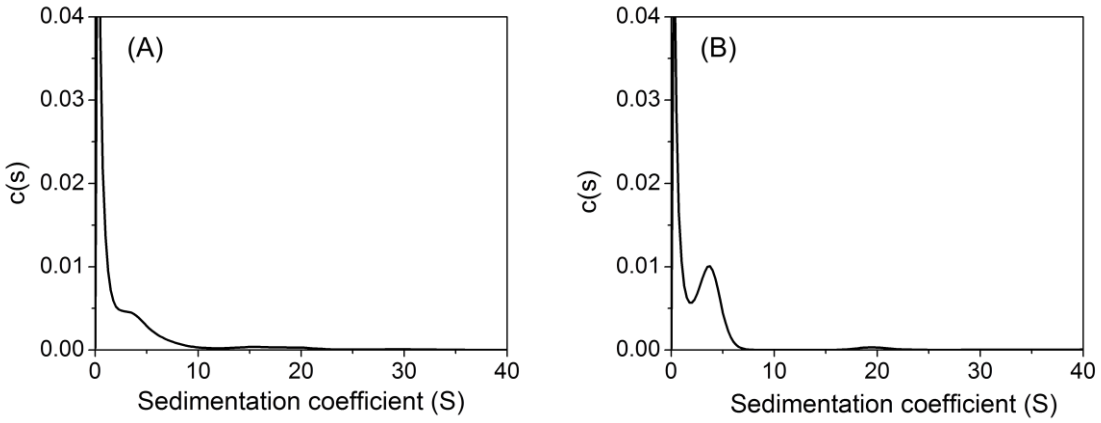

Figure S1. Sedimentation coefficient distributions of A) FBS and B) dFBS at 10% in PBS. Results confirm the negligible contribution of FBS components to sedimentation coefficient distributions > 7S.

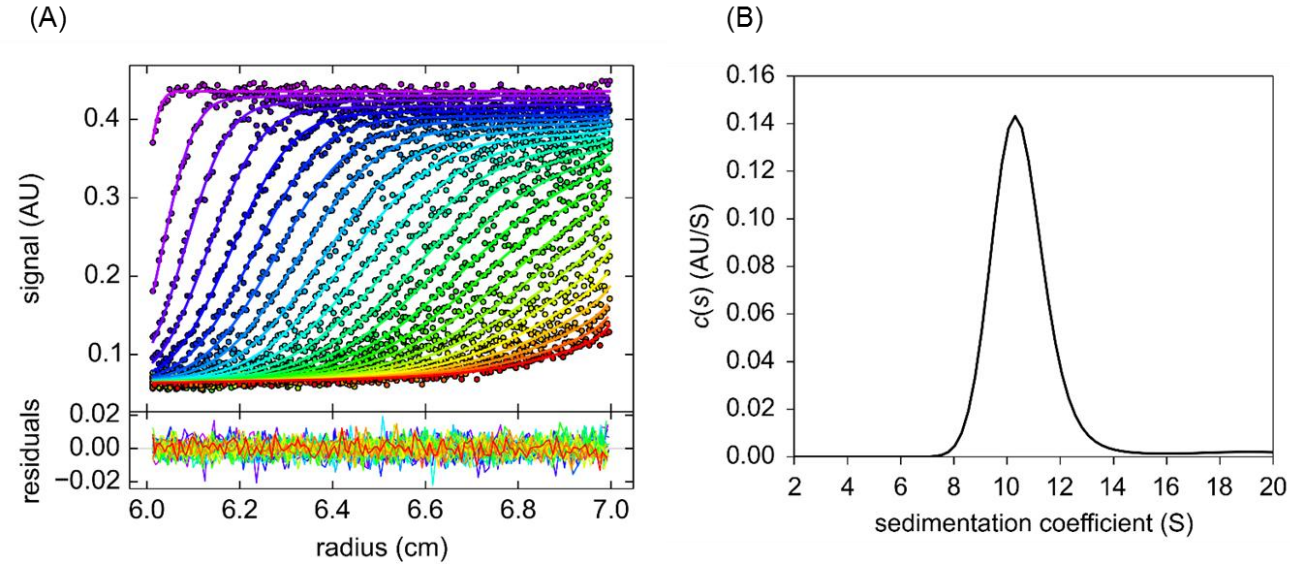

Figure S2. A) Sedimentation velocity profiles for AuGSH-1.4 (higher panel). The best-fit Lamm equation solutions are shown as solid lines. The residuals with an rmsd = 0.004904 OD (lower panel). B) Resulting sedimentation coefficient distributions.

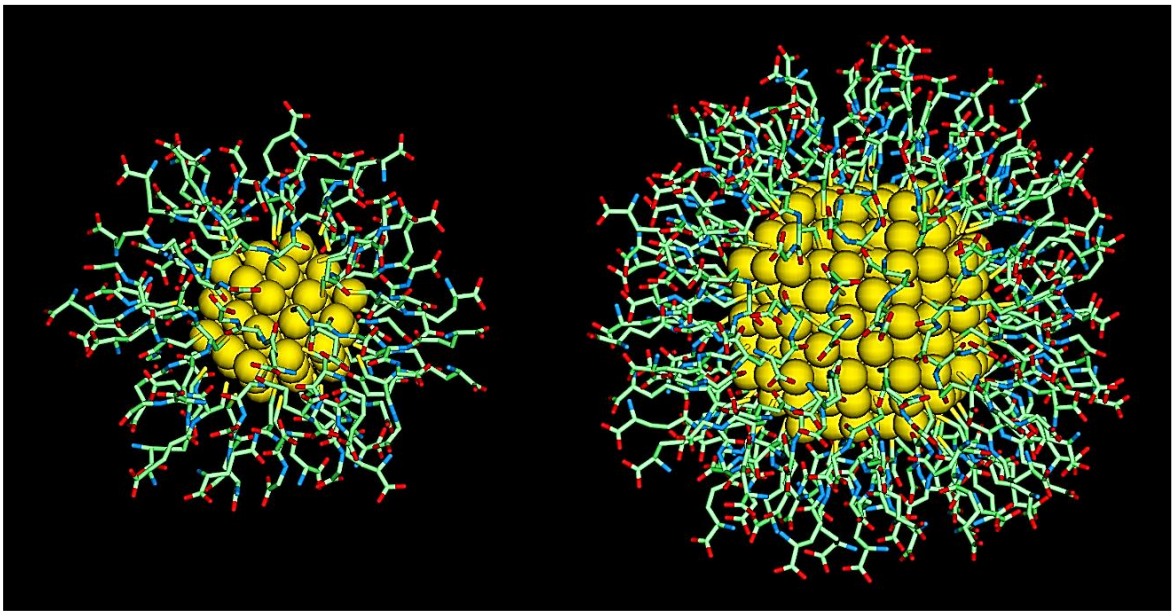

Figure S3: Initial configuration of NP cores and layer of GSH molecules used in the simulations

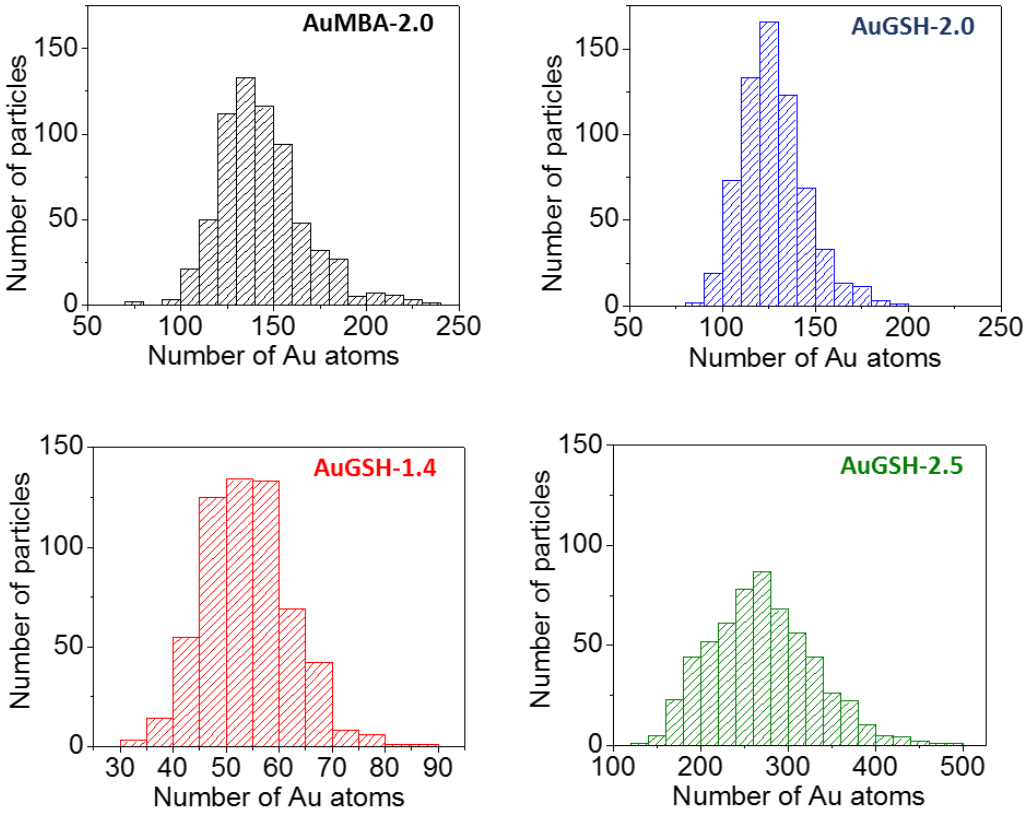

Figure S4. Histograms of STEM measurements of numbers of core Au atoms.

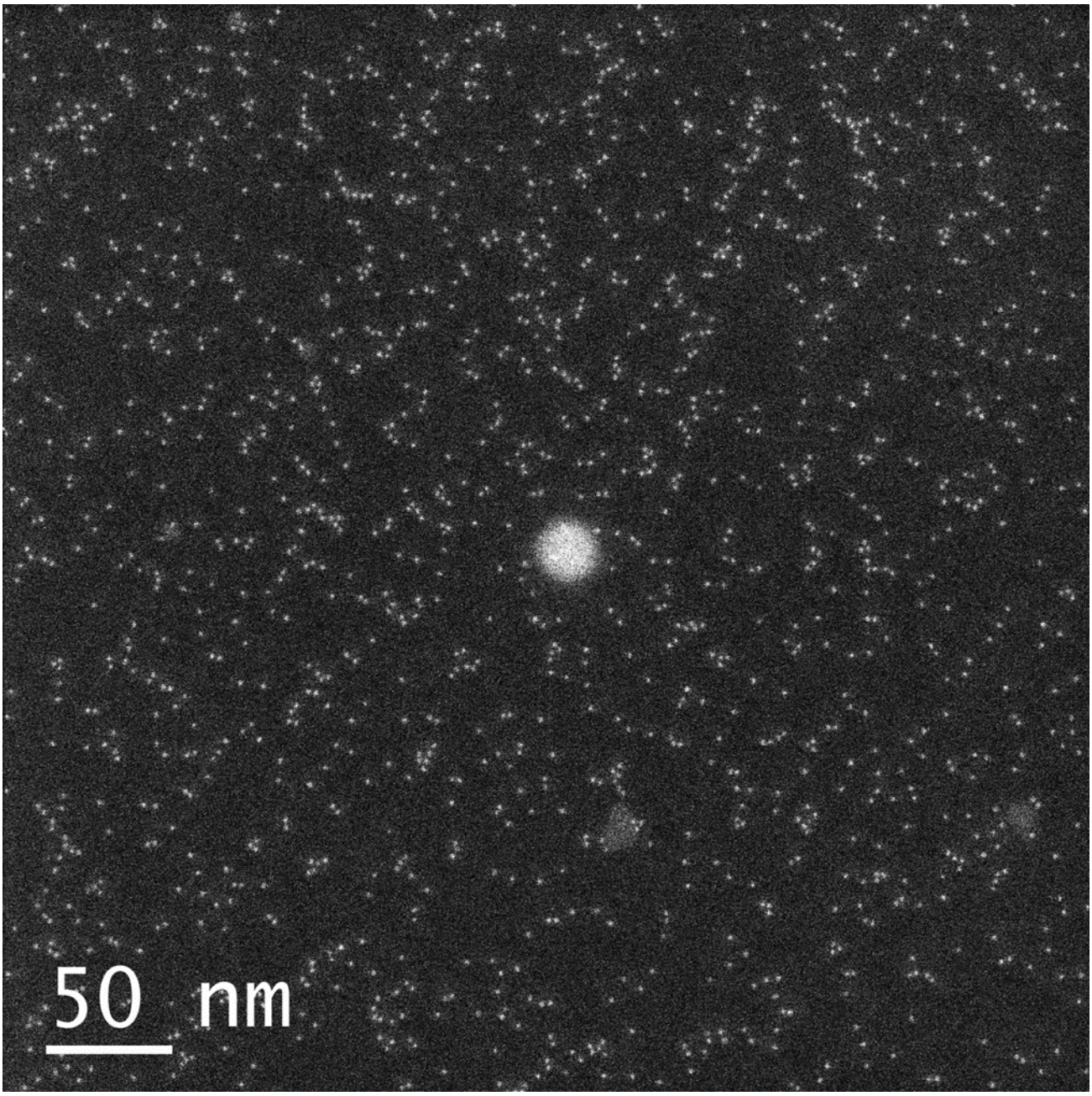

Figure S5. Large field of view STEM image of AuGSH-1.4.

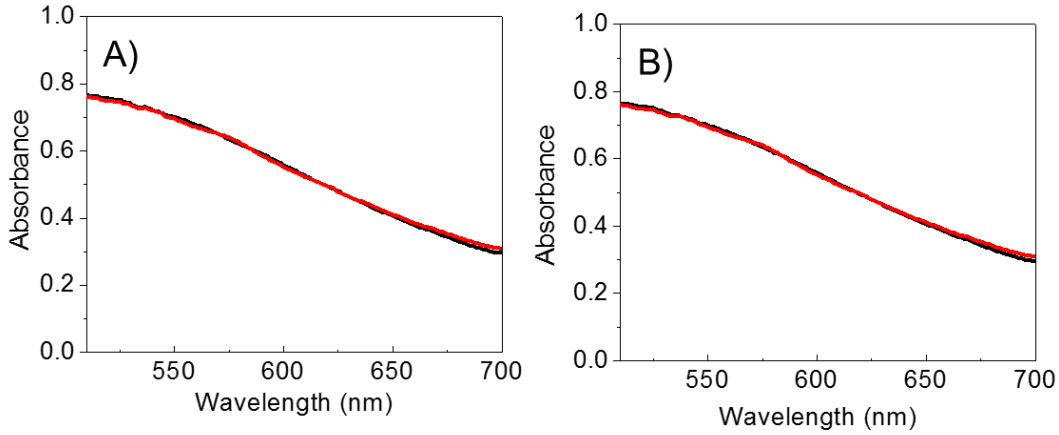

Figure S6. UV-vis analysis of (A) AuMBA-2.0 and (B) AuGSH-2.0 in 50% dFBS-PBS. dFBS consists of serum proteins of molecular weight higher than 10 kDa in 150 mM NaCl. Coinciding absorbance spectra of AuNPs in PBS (black traces) vs. dFBS-PBS (red traces) suggests lack of nanoparticle aggregation in dFBS.

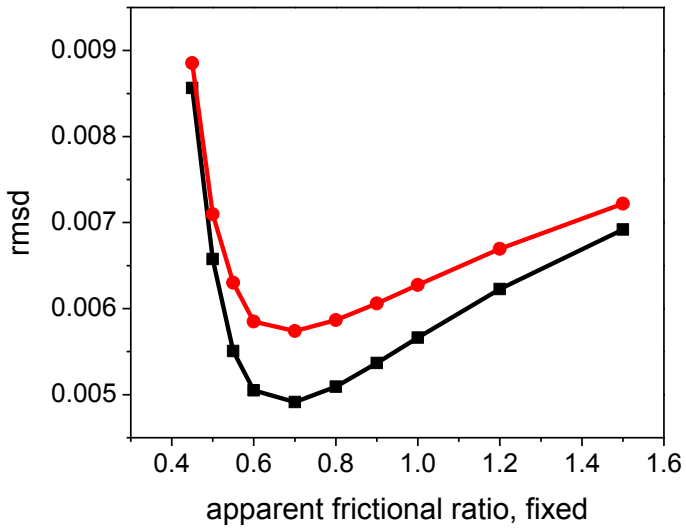

Fig. S7. A theoretical possibility for the coinciding sedimentation velocity of AuGSH-1.4 with/without FBS could be binding of protein coupled with oligomerization. In this case, the increased friction from binding of proteins at the AuNP surface would be compensated for by an increased mass of the oligomerized particle. This can be tested by an analysis of the average friction coefficient of the particles in solution. Shown here is the error surface of the c(s) fit as a function of average frictional ratio. It can be discerned that the frictional coefficient both in the presence and absence of FBS is well defined from the c(s) analysis, and that the particles have the same frictional coefficient in both conditions. This excludes coupled binding and oligomerization as an explanation for an unchanged sedimentation velocity, and confirms the absence of AuGSH-1.4 interactions with FBS proteins as suggested by their unchanged sedimentation coefficient. Black, AuNPs in PBS; red, AuNPs in FBS-PBS.

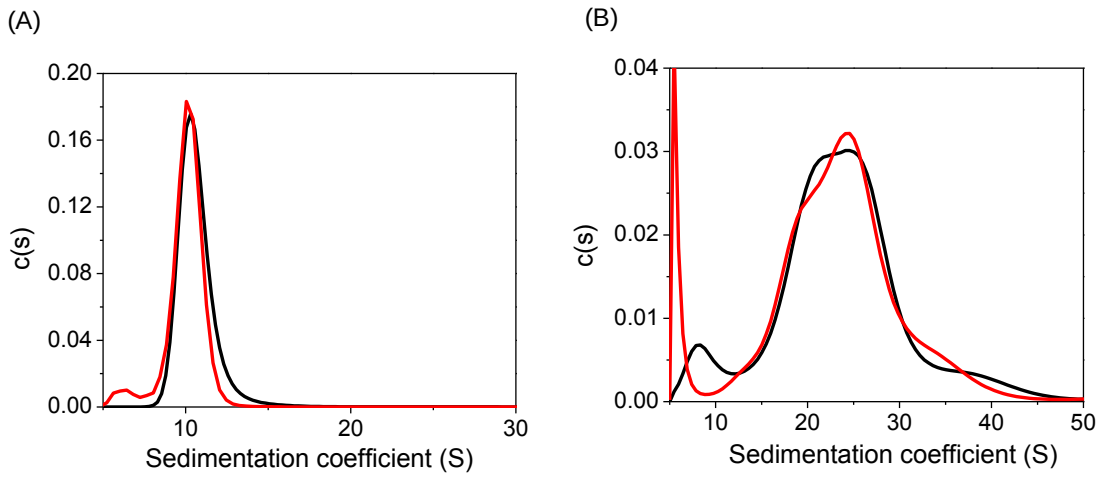

Figure S8. Analytical ultracentrifugation analysis of (a) AuGSH-1.4 and (b) AuGSH-2.5 in PBS supplemented with dialyzed FBS. No signs of aggregation or serum protein interactions are observed for both nanoparticles. Black traces, AuNPs in PBS; red, AuNPs in 10% dFBS-PBS.

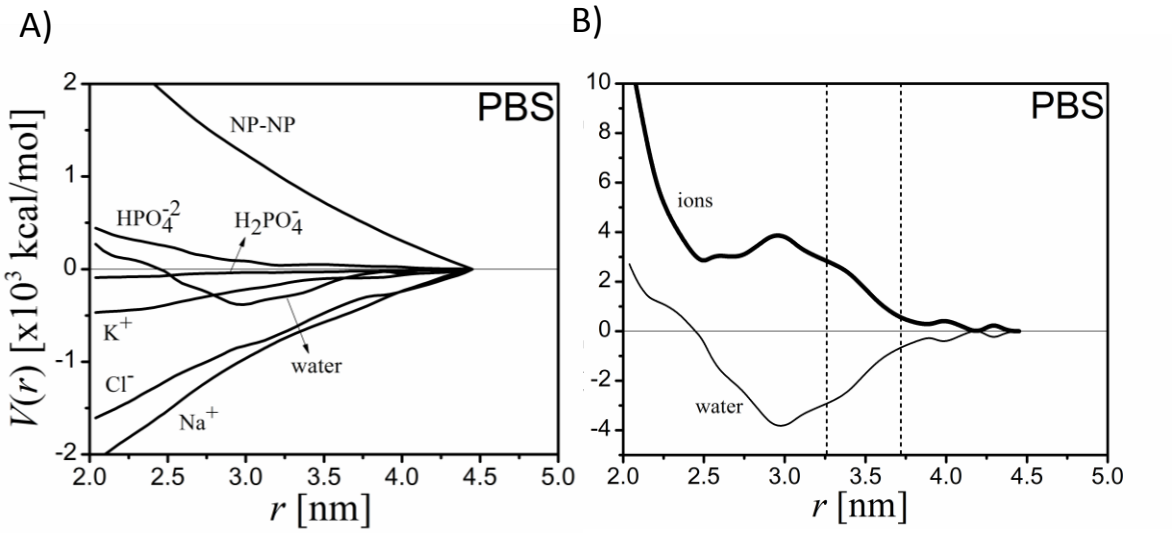

Figure S9: (A) Contributions of all the components of PBS to the PMF of AuGSH-1.4 NP pairs shown in Fig. 8a (red); similar for AuGSH-2.5 (not shown). The direct NP-NP interactions and the Na^+ contributions are scaled by an additional factor of 10. (B) The contribution of all the ions (with the NP-NP added) and water shows that the minima of the potential at r_c and r_s (doted vertical lines) emerge as a complex interplay of opposite forces not related to any individual component.

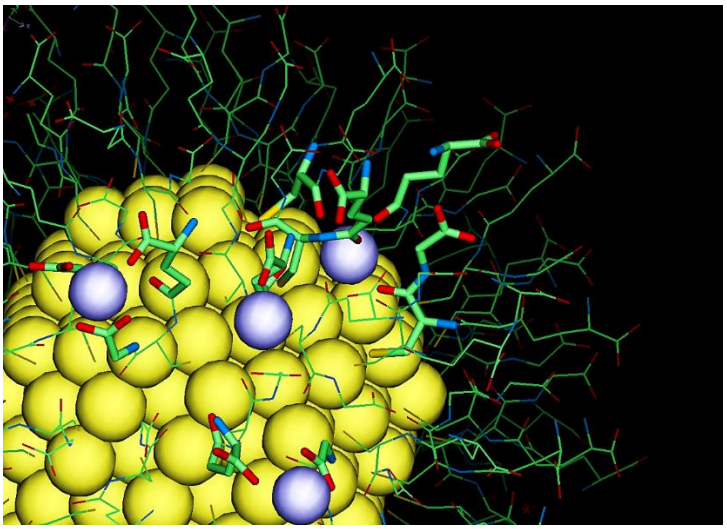

Figure S10: Snapshot from the simulation of AuGSH-2.5 in aqueous $CaCl_2$ solutions at a 8 mM concentration showing strong association of Ca^{2+} ions (white van der Waals spheres) with the passivating layer, forming strong coordination with CO_2^- surface groups not seen with monovalent ions. In contrast, AuGSH-1.4 NPs do not bind Ca^{2+} indicating a qualitatively different behavior of the medium with NP size.